Charge-Transfer Collisions Involving Electron Transfer to Excited States*

Julius Perel and Howard L. Daley
Electro-Optical Systems, Pasadena, California 91107
(Received 9 July 1970; revised manuscript received 28 December 1970)

A crossed-beam technique was used to measure total nonresonant charge-transfer cross sections of the following reactions over an energy range from about 0.5 to 20 keV: $Li^+ + Cs \rightarrow Li + Cs^+$, $Li^+ + Rb \rightarrow Li + Rb^+$, $Li^+ + K \rightarrow Li + K^+$, $Hg^+ + Cs \rightarrow Hg + Cs^+$. For each reaction, the minimum energy defect occurs for transfer to an excited state. The cross sections show typical nonresonant characteristics with the measured maxima corresponding to these energy defects. The production of photons resulting from deexcitation of the Li ($2p$) state formed by charge-transfer collisions was also measured over the same energy range for the reactions involving Li. These photon cross sections (with larger experimental uncertainties than the total cross sections) were "normalized" to the total cross section in the near-adiabatic region using semiempirical relationships. Transfer to an excited state is the dominant channel in the near-adiabatic region with transfer to the ground state becoming increasingly important with increasing impact velocity. The discussion of the $Hg^+ + Cs$ results includes statistical weight considerations.

INTRODUCTION

Total nonresonant-charge-transfer cross sections for ions and atoms of different atomic species are strongly dependent upon the change in potential energy of the transferred electron, the energy defect from resonance (ΔE). This strong dependence exists even when the kinetic energy of the two colliding particles is several orders of magnitude greater than the energy defect. The typical nonresonant cross section is small at low velocities and increases exponentially with increasing velocity (i.e., the near-adiabatic region). The cross section levels off to a broad maximum, then decreases with increasing velocity. In the velocity range above the maximum the nonresonant cross section ($B^+ + A \rightarrow B + A^+ + \Delta E$) approaches the resonant cross section of the incident atom ($A^+ + A \rightarrow A + A^+$) which is typically large at low impact velocities and decreases with increasing velocity.

Hasted[1] used the adiabatic criterion introduced by Massey[2] to approximate the relationship between the velocity at the nonresonant maximum and the energy defect. Agreement between the velocity predictions and experimental data was good for large energy defect cases but not for small energy defect (near-resonant) cases. Rapp and Francis[3] computed cross sections which clearly show the general relationship between the resonant and nonresonant cross sections. The nonresonant cross section was characterized using the energy defect and the "average" ionization potential of the two atoms involved. Predictions of the value and velocity at the cross-section maximum were also in reasonably good agreement with experimental data.

Measurements of resonant and nonresonant cross sections made in our laboratory[4–7] substantiate the predictions of Rapp and Francis if the incident atom resonant cross section is used rather than the one corresponding to an "average" ionization-potential atom. Their predictions also suggest that nonresonant charge transfer in the near-adiabatic region is dominated by transfer to that state which minimizes the energy defect.

Large cross sections at low energies were measured for transfer to an excited state using photon detection techniques[8,9] and for transfer to all states using beam attenuation techniques[10] for the reaction $H^+ + Cs \rightarrow H + Cs^+$. The large values of the cross section at low energies indicated the dominance of transfer to excited states ($\Delta E = 0.50$ eV) over that to the ground state where $\Delta E = 10.70$ eV. For similar type reactions, total cross-section measurements involving He^+ and Ar^+ on K, Rb, and Cs made by Peterson and Lorents[11] were also large at low energies, indicating that transfer to any of several excited states with very small energy defects occurred. Large cross sections were also obtained by Schlacter *et al.*[12] for $He^+ + Cs$, indicating transfer to excited states but with cross sections below those of Peterson and Lorents. No photon measurements were made in either investigation.

The results presented in this paper are for both total cross sections and cross sections obtained from photon measurements for transfer of an electron from a ground state to an excited state with an energy defect which is smaller than ground-state to ground-state transfer. When this occurs, the cross section for transfer to that excited state is strongly dominant in the near-adiabatic region. Initial results of some of these measurements were previously reported by the authors.[13–16]

ANALYTICAL AND EMPIRICAL CONSIDERATIONS

In order to analyze the experimental results several features of the nonresonant-charge-transfer cross section are discussed and summarized. These features include a semiempirical relationship between the velocity at the cross-section maximum and the absolute value of the energy defect with the sign of the energy defect primarily affecting the cross section at low velocities. Also included is a relationship between resonant and nonresonant cross sections and aspects of the competition between alternate final states of the transferred electron.

Hasted[1] used the Massey criterion[2] to show that the velocity at the cross-section maximum (v_m) as given by

$$v_m \approx |\Delta E| a/h \tag{1}$$

shows good correlation with a large number of experimental cases. Difficulties arise in selecting a value of a to be used in Eq. (1), particularly for collisions involving small energy defects.

According to Drukarev[17] (who used a Born approximation), for small energy defects ($\Delta E \ll I$) the value of a to be used in Eq. (1) is proportional to $(2I)^{-1/2}$, where I is the ionization potential. For large energy defects ($\Delta E \approx I$), he predicted a parabolic dependence given by

$$v_m \propto (|\Delta E|)^{1/2} . \tag{2}$$

Incorporating these concepts we have chosen a parametric variation for v_m given by

$$v_m = f(|\Delta E|/I_A^{1/2}) , \tag{3}$$

where I_A is the ionization potential of the incident atom, or more generally, the binding energy of the electron in the initial state. Figure 1 is a plot of v_m vs $|\Delta E|/I_A^{1/2}$ for measurements displaying clear maxima and extrapolations of measurements which do not reach a maximum in the measured velocity range. The extrapolations are generally made by assuming that maxima occur when the smoothly varying part of the exponentially increasing nonresonant cross section levels off to approximately 90% of the symmetric resonant cross section of the incident neutral atom. This empirically obtained value appears valid over a range of ±20%, based upon experimental uncertainties including the differences between results obtained at various laboratories. Other requirements and/or exceptions to these generalizations are discussed later.

The data in Fig. 1 show two different functional dependences in accordance with Eqs. (1) and (2). At very low values of $|\Delta E|/I_A^{1/2}$, a linear relationship conforming with the adiabatic criterion is seen (as also predicted by Drukarev). For values of $|\Delta E|/I_A^{1/2} > 0.15(\text{eV})^{1/2}$ a parabolic dependence occurs, extending to much lower energy defects than indicated by Drukarev. A listing of the data plotted in Fig. 1 is given in Table I which provides the minimum energy defect assuming all incident particles are in the ground states, and the measured, extrapolated, or predicted velocity at the maximum, plus references for the measured reactions. Reactions are coupled in conjugate pairs (interchanged incident ions and atoms) and include those involving excited final states. When an excited final state is involved, $|\Delta E|$ is not the same for conjugate reactions, resulting in very different cross-section curves. Conversely, when only ground final states are involved, the cross sections for conjugate pairs are very similar for these low energy defect reactions[3] except in the very low impact velocity region where the sign of ΔE becomes important. An examination of experimental data indicates that cross-section extrapolations to zero velocity approach zero for negative-energy-defect cases and

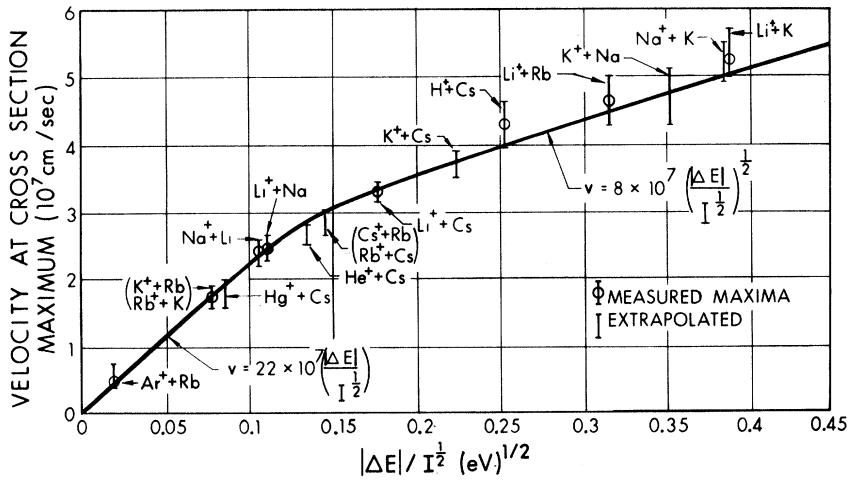

FIG. 1. Plot of the velocity at the cross-section maximum (v_m) as a function of $|\Delta E|/I^{1/2}$. Most of the data shown are the experimental results of the authors. The equations are empirical and in agreement with measurements made in other laboratories at higher values of $|\Delta E|/I^{1/2}$. Table I contains a listing of the data used.

TABLE I. Velocity at cross-section maximum (v_m) and associated energy defect (ΔE) for reaction data used in Fig. 1.

Reaction	ΔE[a] (eV)	v_m (10^7 cm/sec)	Reference
$Rb^+ + K \rightarrow Rb + K^+$	−0.16	1.7	6
$K^+ + Rb \rightarrow K + Rb^+$	0.16	1.7	5
$Hg^+ + Cs \rightarrow Hg(6p\,^1P_1^0) + Cs^+$	−0.17	1.7[b]	13, 15, present paper
$Cs^+ + Hg \rightarrow Cs + Hg^+$	−6.54	11[c]	
$Na^+ + Li \rightarrow Na + Li^+$	−0.25	2.3	7
$Li^+ + Na \rightarrow Li + Na^+$	0.25	2.4	7
$Cs^+ + Rb \rightarrow Cs + Rb^+$	−0.28	2.8[b]	4, 18
$Rb^+ + Cs \rightarrow Rb + Cs^+$	0.28	2.8[b]	4, 18–20
$Li^+ + Cs \rightarrow Li(2p) + Cs^+$	−0.35	3.3	14, 19, present paper
$Cs^+ + Li \rightarrow Cs + Li^+$	−1.50	7.3[c]	14, present paper
$K^+ + Cs \rightarrow K + Cs^+$	0.45	3.6[b]	18–21
$Cs^+ + K \rightarrow Cs + K^+$	−0.45	3.7[c]	18
$Li^+ + Rb \rightarrow Li(2p) + Rb^+$	−0.63	4.6	16, present paper
$Rb^+ + Li \rightarrow Rb + Li^+$	−1.21	6.4[c]	
$K^+ + Na \rightarrow K + Na^+$	−0.80	4.7[b]	22
$Na^+ + K \rightarrow Na + K^+$	0.80	5.2[b]	6
$Li^+ + K \rightarrow Li(2p) + K^+$	−0.80	5.3	present paper
$K^+ + Li \rightarrow K + Li^+$	−1.05	5.7[c]	
$Na^+ + Cs \rightarrow Na(3p) + Cs^+$	−0.86	4.5/5.4[c]	18, 19
$Cs^+ + Na \rightarrow Cs + Na^+$	−1.25	5.8[c]	18
$Na^+ + Rb \rightarrow Na + Rb^+$	0.96	5.6[c]	
$Rb^+ + Na \rightarrow Rb + Na^+$	−0.96	6.3[c]	
$H^+ + Cs \rightarrow H(2s, 2p) + Cs$	−0.50	4.3	8–10
$Cs^+ + H \rightarrow Cs + H^+$	−10.70	13.5[c]	
$He^+ + Cs \rightarrow He + Cs^+$	~0.64[d]	~2.6	11, 12
$Cs^+ + He \rightarrow Cs + He^+$	−20.7	~33[c]	
$Ar^+ + Rb \rightarrow Ar + Rb^+$	~0.04[d]	0.5	11
$Rb^+ + Ar \rightarrow Rb + Ar^+$	−11.6	13.6	

[a]Data taken from C. E. Moore, *Atomic Energy Levels*, Natl. Bur. Std., Circular No. 467 (U.S. GPO, Washington, D. C., 1949), Vol. 1; (1952), Vol. 2; (1958), Vol. 3.

[b]Extrapolated experimental results.

[c]Predicted using Fig. 7 and equation for higher values of $(\Delta E/I_A)^{1/2}$.

[d]Unspecified final state.

approach a nonzero cross section for positive-energy-defect cases.[5,11,18,19] The difference shows up clearly for conjugate reactions where the energy defects have the same absolute values but opposite signs.[4,6,7,18,23,24]

To characterize the dominance of transfer to a given final state, a competitive factor, taken as the ratio of the two energy defects for competing final states, is used. This factor is defined as the ratio of the minimum energy defect to the next larger one. A value of 1 indicates equal competition whereas values less than 1 indicate reduced competition. For sufficiently low ratios, transfer to the state involving the smallest energy defect provides the dominant contribution to the total cross section in the near-adiabatic region. This concept provided a basis for the "normalization" of the photon measurements reported here.

From our measured cross sections and an examination of the theoretical and experimental results of others, several features of the nonresonant cross sections have been abstracted. These features correspond very well with alkali-metal data, and low-energy-defect data in general. In any case the use of these features as aids in understanding the nonresonant-charge-transfer process have revealed important aspects of the process that are not readily obvious. Although work in extending these considerations to all charge-transfer results is still in process, a listing of "semiempirical relationships" are given below which have been useful in the analysis of nonresonant charge transfer.

(a) The important (or minimum) energy defect can be determined from a comparison of the binding energy levels of the incident and product atoms.

(b) The velocity at the maximum of the cross section corresponding with the energy defect can be obtained using Fig. 1 where the value of I_A to be used is the binding energy of the electron in its initial state.

(c) The cross-section value at the maximum is less than the value of the incident atom resonant cross section at the same velocity. The empirical 90% criterion obtained for the alkali metals appears

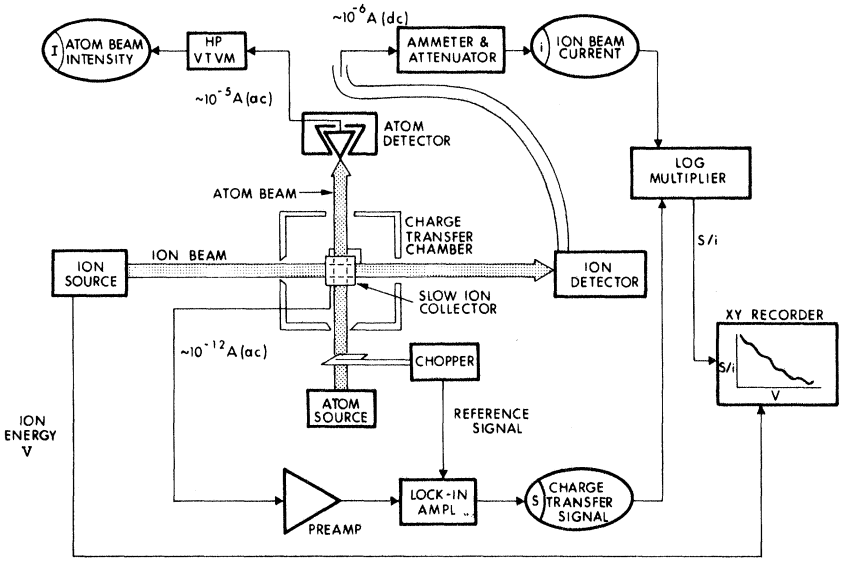

FIG. 2. Schematic diagram of the experimental technique for the measurement of total charge-transfer cross sections. For the photon measurements the charge-transfer chamber is removed and the crossed-beam region is observed using a photomultiplier. In each case the modulated signal produced by the chopped atom beam is amplified and compared to a synchronized reference signal at the lock-in amplifier. The ratio of the charge-transfer signal and the ion beam current is obtained using the log multiplier and plotted as a function of the ion beam energy using the XY recorder.

valid within the limitations imposed by the statistical weights of the states involved.

(d) For velocities below the velocity at the maximum the cross section shows the typical near-adiabatic behavior with transfer to that state having the minimal energy defect providing the dominant contribution.

(e) For velocities greater than the velocity at the maximum the cross section approaches the symmetric-resonant cross section of the incident atom.

EXPERIMENTAL METHOD

Crossed-beam techniques were used to measure total charge-transfer cross sections and the production of photons resulting from collisions over an approximate energy range 0.5–20 keV. The photon signal as a function of velocity was "normalized" to the total cross section in the near-adiabatic region to obtain the absolute cross section for electron transfer to the first excited state of Li.

The experimental arrangement, shown schematically in Fig. 2 for the total cross-section measurements, was described in detail previously[4] and also includes provisions for oxygenation of the atom detector and the ion source. Li^+ ion beams were generated using surface-ionization techniques and detected using Faraday cups. The Hg^+ ion beam was generated using an electron-bombardment ion source. The atom beams, formed by the collimation of the alkali-metal vapor diffusing from a heated reservoir, were modulated at 30 Hz using a slotted cylinder with the atom beam intensity measured using surface-ionization techniques. Slow ions produced by charge-transfer collisions in the beam interaction region were swept to a collector plate by a small electric field. This modulated slow-ion current was amplified, frequency-selected, and measured using the lock-in amplifier whose reference signal was synchronized with the atom beam modulation system. For the photon measurements, the charge-transfer chamber was removed and the beam intersection region was monitored using a photomultiplier in conjunction with a monochromator or with filters to detect the photons produced in charge-transfer collisions. The modulated photon signal was processed just as the slow-ion current was in the total cross-section measurements.

At a given ion energy (ion source voltage), the ion beam current (i), the atom beam intensity (I), and the charge-transfer signal (S) were measured as well as the temperature of the atom source exit aperture. From this data and the dimensions of the interaction region, absolute cross sections can be calculated using

$$\sigma = e v_a w (S/iI) , \tag{4}$$

where e is the charge of the electron, v_a is the atom mean velocity in the reservoir,[4] and w is the pertinent interaction-region dimension. For the total cross-section measurements, the charge-transfer signal (S) was the slow-ion current to the collector plate. For the photon measurements, S was proportional to the number of photons produced in the interaction region.

Ion Beam System

The Li ion source used in this investigation utilized direct surface ionization from a continuously oxygenated porous tungsten ionizer to generate ground-state ions. The source configuration and performance are described in Ref. 25. The Hg^+ ion source was of the low-pressure electron-bombardment type.[26,27] Prior to the cross-section measurements, the Hg source was operated over

a wide range of operational parameters, such as discharge voltage and magnetic field combinations, to establish the optimum discharge mode for the production of singly ionized ground-state ions while minimizing the formation of excited ions and/or doubly ionized Hg ions. From the data of Bleakney,[28] and later confirmed at this laboratory using time-of-flight mass-spectroscopy techniques,[29] the percentage of Hg^{++} generated by our ion source was estimated at 4% or less, so that the Hg^{++} present in the beam did not significantly affect the experimental results.

Ion beam currents of $10^{-7}-10^{-6}$ A were measured using a Faraday cup for the total cross-section measurements. The ion beam was highly collimated prior to the charge-transfer chamber with the Faraday cup 2.5 cm diam by 12.5 cm long and having no grids. For this geometry there is negligible error due to the loss of secondary electrons in the ion current measurements. For the photon measurements, the interaction region was substantially increased in volume by widening apertures to enlarge both ion and atom beam dimensions. The Faraday cup used to measure the ion beam current in these measurements was about 7.5 cm diam with two grids (the first at ground and the second at about -50 V) used to suppress secondary electrons. The grids were made by spot welding 0.005-cm-diam tungsten wires across support structures to give >90% transparency. Typical ion current intensities were $10^{-4}-10^{-3}$ A.

Retarding potential measurements were made at several ion-accelerating voltages and showed an energy spread ~2% of the beam energy.

Atom Beam System

Ground-state atom beams were generated by the collimation of alkali-metal vapor effusing from a 0.1-cm-diam circular exit aperture in a heated reservoir. For the total cross-section measurements, the atom beam was approximately three times wider than the ion beam. Care was taken to ensure that all of the ion beam passed through the atom beam. For this condition the critical interaction dimension (w) in Eq. (4) was the atom beam width which was constant over a wide range of atom beam intensities as determined using a moveable surface-ionization detector. The entire atom beam was monitored with the detection system and associated testing identical to those described in Ref. 4 except for measurements involving K where oxygenation was used to ensure that the detection efficiency was virtually 100%. The desorption time data obtained for K (as well as that for Li and Na) have been reported.[30] Typical atom beam detection signals were 10^{-5} A, corresponding to beam intensities of 6×10^{13} atoms/sec.

Because the interaction volume was enlarged for the photon measurements, only a fraction of the total atom beam was measured using a 0.25-cm-wide $\times$2.5-cm-long$\times$0.002-cm tungsten ribbon. Typical values of I/w [Eq. (4)] were equivalent to $\sim10^{15}$ atoms/cm sec.

Detection Systems

The detection system used in the total cross-section measurements and associated testing was described in Ref. 4 except for the use of a log multiplier circuit[31] which permitted direct high-resolution plotting of relative cross sections. This relative curve was then correlated with absolute values of the cross section obtained at several ion energies with an estimated uncertainty of $\pm10\%$. Typical values of the charge-transfer signal (i.e., the slow-ion current to the collection plates) were $10^{-10}-10^{-12}$ A.

The detection system for the photon measurements utilized a liquid-nitrogen-cooled photomultiplier with an S-1 spectral response in conjunction with a scanning monochrometer or filter combinations. Other than this change, the same instrumentation was used as for the total cross-section measurements with the relative cross section now the ratio of the photomultiplier output to the measured ion current at a constant atom beam intensity. The correlation of the high-resolution relative cross sections to absolute cross sections involved the spectral responsivity of the detector, the gain of the signal amplification system, and the effective solid angle seen by the photomultiplier. The major uncertainty was the solid angle observed by the photomultiplier and only order-of-magnitude absolute cross sections were obtained. Typical values of the number of photons detected were 10^5-10^7 photons/sec.

The spectral distribution of the photon signal was examined using various optical filter combinations or a 0.5-m Ebert mount scanning monochromator. Using the monochromator, the wavelength region from approximately 4000 to 8000 Å was examined with the only detectable signal occurring at 6708 Å, which corresponds to the first excited state of Li. Other signals having intensities greater than 10% of the signal at 6708 Å would have been detectable in this wavelength region. The measurements made using various filter combinations were identical in curve shape to those made with the monochromator and those made with no filters. The difference in signal levels (with and without filters) corresponded to the transmission attenuation of the filter combinations used. A filter combination having bandpass of about 200-Å full width at half-maximum encompassing the 6708-A wavelength was the narrowest used.

In all photon measurements, the signal levels were maximized for ion velocities corresponding

to the velocity near the cross-section maximum. The velocity-dependent error resulting from the lifetime of the excited state and the fixed field of view of the detector was computed and used to compensate the measured photon signal.

RESULTS AND ANALYSIS

Four reactions were measured in which electron transfer to an excited state is the dominant process. These reactions are listed showing the excited final states and the ground states where they are considered important in the measured range:

$$Li^+ + Cs \rightarrow Li\,(2p) + Cs^+ - 0.35\ eV \rightarrow Li + Cs^+ + 1.50\ eV\,, \quad (5)$$

$$Li^+ + Rb \rightarrow Li\,(2p) + Rb^+ - 0.63\ eV \rightarrow Li + Rb^+ + 1.21\ eV\,, \quad (6)$$

$$Li^+ + K \rightarrow Li(2p) + K^+ - 0.80\ eV \rightarrow Li + K^+ + 1.05\ eV\,, \quad (7)$$

$$Hg^+ + Cs \rightarrow Hg\,(6p'P_1^0) + Cs^+ - 0.17\ eV\,. \quad (8)$$

The energy defects listed are the difference between the binding energies of the given final state and the initial (ground) state of the neutral atoms involved. The ground-state energy defects for these reactions are sufficiently large that transfer to excited states is dominant over much of the measured energy range and strongly dominant in the near-adiabatic region. The energy defect for transfer to the ground state for reaction (8) is 6.54 eV, which is much too large to be important in the measured velocity range. The various energy defects are illustrated in Fig. 3 which shows binding energy diagrams for the four reactions. The electron is shown transferring from the ground state of the incident atom to the state of the product atom resulting in the minimum energy defect. Transfer

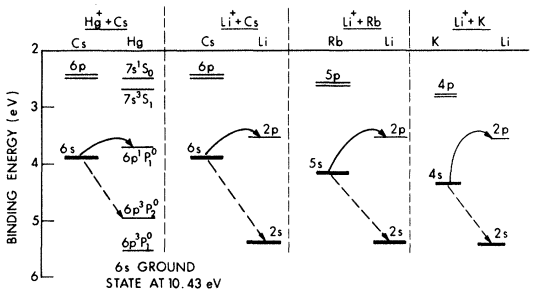

FIG. 3. A schematic representation of electron transfer between the binding energy levels of the incident atoms and product atoms is shown for the four reactions reported. The ionization level is taken as zero for this energy-level diagram and that path minimizing the energy defect is shown. Competitive paths are also shown for the next larger energy defects.

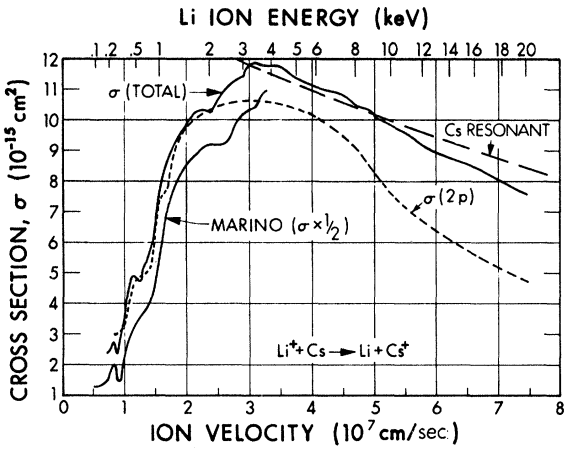

FIG. 4. Li + Cs total charge-transfer cross sections and the $\sigma(2p)$ cross sections for transfer to the Li(2p) state as a function of ion velocity. The total cross-section results of Marino (Ref. 19) are nearly twice the present measurement, but the two are in good agreement in shape and structure. Also shown is the extrapolated Cs resonant cross section (Ref. 4).

to other states can occur but with lower probability because of larger energy defects. Greater competition exists between the ground state and the excited state for reaction (7) since the absolute value of these two energy defects are closer to each other than those of reactions (5), (6), and (8). Statistical weight considerations are also important in nonresonant charge transfer to determine allowed channels which can result in electron transfer. For reactions (5)–(7), the configurations of the incident and product states are the same so that the energy defect is the more significant consideration. For $Hg^+ + Cs$ [reaction (8)] the state configurations are different from those in the other three reactions and will be discussed with the experimental results.

Regular oscillatory structure similar to that observed in other alkali-metal charge-transfer cross sections[23] also occur in some of the results reported here. The structure becomes less evident with increasing competitive factor (ratio of the smallest to the next larger energy defect). The structure is clearly seen in $Hg^+ + Cs$; is less clear in $Li^+ + Cs$; is barely discernable in $Li^+ + Rb$; is not observed in $Li^+ + K$.

$Li^+ + Cs$

The total charge-transfer cross section σ (total) for $Li^+ + Cs$ shown in Fig. 4 displays the typical nonresonant characteristics. The results of Marino[19] are in good agreement in curveshape and structural details; however his cross sections are nearly twice the values of the present investigation. At the velocity of the maximum and above, our total cross section is close to the extrapolated Cs

resonant cross section[4,32] (also shown in the figure). The extrapolation is based upon the typical resonant behavior given by $\sigma = A - B \ln v$, where v is the impact velocity. The velocity at the nonresonant cross-section maximum follows the empirical relationship shown in Fig. 1 when the energy defect for transfer to the Li ($2p$) state is used.

The measurement of photon production resulting from the deexcitation of the Li ($2p$) state as a function of the ion velocity yielded an absolute cross section for electron transfer to the $2p$ state, but with larger uncertainty than for the total cross-section measurements. Order-of-magnitude agreement with the total cross section in the near-adiabatic region was obtained. To reduce the uncertainty in the photon measurements a normalization technique was used which was based upon the semiempirical relationships listed previously. The competitive factor $[|\Delta E(2p)|/|\Delta E(2s)|]$ is 0.23 for this reaction, indicating very low competition in the near-adiabatic region, so that transfer to the $2p$ state is strongly dominant over that to the ground state. The extent of the dominance was further indicated by the similarity in curve shapes between the total cross section and the photon curve over most of the near-adiabatic region. The normalization consisted of shifting the cross-section values within the uncertainty of the photon data and without altering the relative curve shape, so that they approximate but do not exceed σ(total) in the near-adiabatic region. The result of this normalization is the $\sigma(2p)$ curve in Fig. 4. Note that the maximum at the $\sigma(2p)$ curve occurs at a slightly lower velocity than that for the total cross section. In addition, the $\sigma(2p)$ cross section decreases more rapidly than the total cross section in the velocity region above the maximum. This reflects the increasing cross section for transfer to the ground state. These general features were also observed with reactions (6) and (7).

To further demonstrate that the $Li^+ + Cs$ reaction is dominated by transfer to an excited state, a measurement was made on the conjugate reaction $Cs^+ + Li \rightarrow Cs + Li^+ - 1.5$ eV where the minimum energy defect occurs for ground-state to ground-state transfer with a predicted maximum at 7×10^7 cm/sec. The $Cs^+ + Li$ cross-section value was at least an order of magnitude below that of $Li^+ + Cs$ at 1.5×10^7 cm/sec. The low cross-section values precluded a determination of curve shape but demonstrated that different energy defects are involved for the two reactions.

The results of the present investigation, including reactions (6) and (7), illustrate the relationships between nonresonant and resonant cross sections, particularly the concept that the nonresonant should not exceed the resonant cross section. However, the absolute values of Marino's results (shown in Fig. 4) exceed extrapolated Cs resonant cross sections. The $He^+ + Cs$, Rb, and K results of Peterson and Lorents[11] also show cross sections that exceed those of the incident atom resonant cross section. These measurements, involving collisions of light ions and heavy atoms, performed by the collection of slow ions in the collision region, are subject to possible error due to ionization and large-angle ion scatter into electrodes with subsequent secondary electron emission (as indicated by Marino). These processes could cause the measured cross section to be too large, particularly at the higher velocities. This may explain the differences between our $Li^+ + Cs$ results and those of Marino since our apparatus discriminates against error due to ionization and secondary electron emission (scattered ions could cause an error but is considered to be within the estimated uncertainty). Similarly, the $He^+ + Cs$, Rb, and K results, which also involve transfer to excited states, show cross sections exceeding those of the incident atom resonant cross sections. These data are subject to the same errors as Marino and may explain the disagreement with the $He^+ + Cs$ results of Schlacter *et al.*[12] which do not exceed the Cs resonant cross section. Schlacter and co-workers' beam attenuation measurements are not subject to these errors.

$Li^+ + Rb$

The $Li^+ + Rb$ determinations are shown in Fig. 5. The total cross-section curve σ(total) displays the typical nonresonant characteristics with the maximum approximately 80% of the extrapolated Rb resonant cross section[4] (also shown in the figure). The velocity at the maximum follows the relationship given in Fig. 1 when the energy defect for transfer

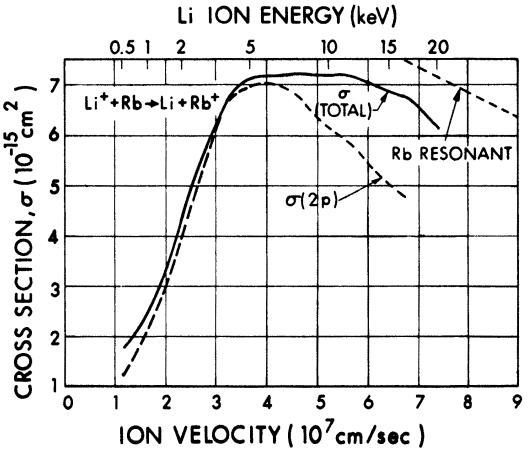

FIG. 5. Li + Rb total charge-transfer cross sections and the $\sigma(2p)$ cross section for capture into the Li($2p$) state of Li as a function of ion velocity. The extrapolated Rb resonant cross section is also included (Ref. 4).

to the Li ($2p$) state is used. For velocities greater than that at the maximum this nonresonant cross-section curve approaches the Rb resonant cross section.

For this reaction transfer to the Li ($2p$) state is also dominant, although somewhat less than for the $Li^+ + Cs$ case since the competitive factor for transfer to the ground state is 0.52. The photon curve was normalized to the total cross-section curve in the same manner as $Li^+ + Cs$ to obtain the absolute cross section for transfer to the $2p$ state $\sigma(2p)$. In this case the narrow maximum clearly occurs at a lower velocity and the cross section decreases more rapidly in the high velocity region than the total cross section. The difference between the two curves is the estimated cross section for transfer to the ground state which has a predicted maximum at 6.2×10^7 cm/sec as computed from the equation in Fig. 1. The broad total cross-section maximum results from the increasing contribution of ground-state transfer with increasing velocity.

$Li^+ + K$

The $Li^+ + K$ results shown in Fig. 6 also display the typical nonresonant characteristics. The total cross section σ(total) shows a well-defined broad maximum of approximately 80% of the extrapolated K resonant cross section[6] with the two curves converging with increasing velocity. The measurements of Pivovar *et al.*,[24] in the velocity range above that shown in Fig. 6, have cross-section values well below the extrapolated K resonant cross section.

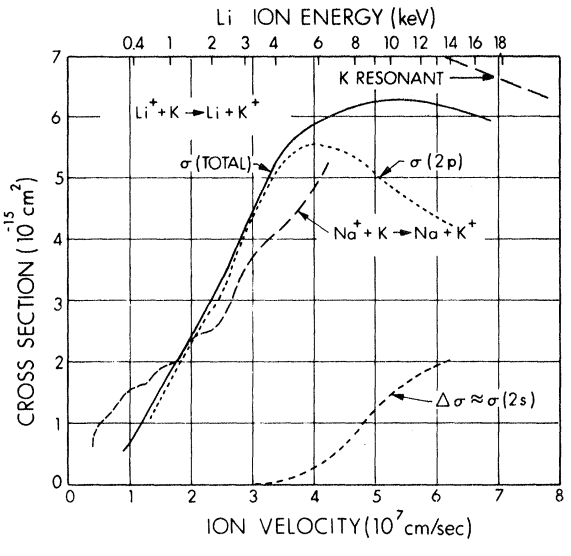

FIG. 6. $Li^+ + K$ total charge-transfer cross sections and $\sigma(2p)$ cross section for capture to the Li($2p$) state as a function of ion velocity. The difference between the two curves ($\Delta\sigma$) is taken to approximate the cross section for transfer to the ground state. The cross sections for $Na^+ + K \rightarrow Na + K^+$, having the same $|\Delta E|$ and incident atom (K) as $Li^+ + K$, and the K resonant cross sections are shown for comparative purposes (Ref. 6).

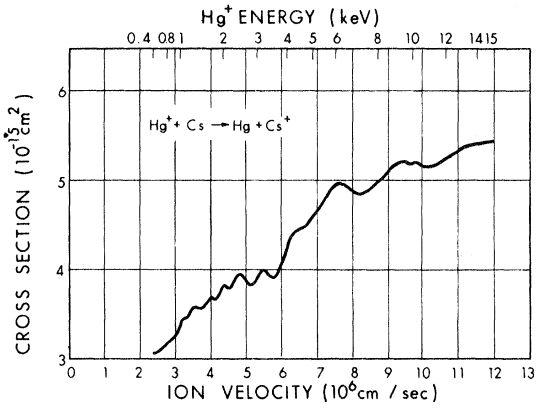

FIG. 7. Charge-transfer cross section vs ion velocity for $Hg^+ + Cs$. The large cross-section values in the measured velocity range provide experimental evidence for electron transfer to an excited state. The characteristics of the oscillatory structure are similar to oscillations found in other alkali-metal charge-transfer cross sections.

The photon measurements were also normalized to give the $\sigma(2p)$ curve shown in Fig. 6. The $\sigma(2p)$ curve has a maximum at a significantly lower velocity and decreases more rapidly in the high velocity region than the total cross section. Transfer to the first excited state is less dominant over the ground state in this reaction with a competitive factor of 0.79, indicating that the stronger competition causes the sharp decrease of the $\sigma(2p)$ curve. The $\Delta\sigma$ curve is the difference between the total and $\sigma(2p)$ cross sections, with transfer to the Li ($2s$) ground state expected to be the dominant component in the energy range shown.

A similarity exists between this reaction and the $Na^+ + K \rightarrow Na + K^+ + 0.80$ eV reaction[6] also shown in Fig. 6. Both reactions have the same incident atom (K) and absolute value of the energy defect ($|\Delta E| = 0.80$ eV). The differences are the sign of the energy defects, the final states, and the competitive ratios. The cross-section values, as expected, are very similar with the differences at the low velocity end of the near-adiabatic region illustrating the effect of the sign of the energy defect.

$Hg^+ + Cs$

The total charge-transfer cross section for $Hg^+ + Cs$ as a function of ion velocity[15] is shown in Fig. 7. Only part of the near-adiabatic region was observed because the heavy ion limited the impact velocity. The cross-section curve appears to be leveling off at higher velocities, indicating the existence of a peak somewhat beyond the measured

range having a cross section of about 45% of the Cs resonant cross section. This extrapolated peak corresponds to transfer to the Hg $(6p^1P_1^0)$ state[33] (the minimum energy defect) from the relationship shown in Fig. 1. The next larger energy defect occurs for transfer to the $6p^3P_2^0$ state with $|\Delta E| = 1.08$ eV. Transfer involving the smallest energy defect is therefore strongly dominant with a competitive ratio for transfer to the next smallest ΔE being

$$|\Delta E(6p^1P_1^0)|/|\Delta E(6p^3P_2^0)| = 0.16 .$$

From statistical weight considerations, the collision of these two incident ground-state particles results in a quasimolecular ion $HgCs^+$ in $^1\Sigma$ and $^3\Sigma$ states with probabilities of $\frac{1}{4}$ and $\frac{3}{4}$, respectively. The $^1\Sigma$ state is a direct channel to the $6p^1P_1^0$ state and for large atoms such as these, spin-orbit coupling provides an additional channel where the $^3\Sigma$ state "borrows" some of the properties of the $^1\Pi$ state, which is also a direct channel to the product particles.[34] As a result, the probability for transfer to the Hg $(6p^1P_1^0)$ state should be larger than that expected for the $^1\Sigma$ channel alone. Thus the cross section at the maximum for transfer to the $6p^1P_1^0$ state should be below the 90% criterion but above 22% of the Cs resonant cross section by an amount dependent upon the contribution from the additional channel. The 45% value at the peak obtained from extrapolation of the data is consistent with these considerations.

From these generalized features of nonresonant cross section, the total cross-section maximum should occur at an ion velocity close to that predicted for the maximum for transfer to the Hg $(6p^3P_2^0)$ state. The $^3\Sigma$ state of $HgCs^+$ with the $\frac{3}{4}$ probability is the direct channel to the product particles for this state and the $^1\Sigma$ state is an additional spin-orbit coupling channel through the $^3\Pi$ product particle state. Thus for velocities above those of our measurements, the total cross section is expected to approach the Cs resonant cross-section curve, with the maximum near 6×10^7 cm/sec and dominated by transfer to the $6p^3P_2^0$ state.

CONCLUSIONS

Several features of the total charge-transfer cross sections and cross sections obtained from photon measurements show that electron transfer to a given excited state can be dominant over all other final states. Evidence for this dominance are (a) the minimum energy defect occurs for transfer to the excited state, (b) cross-section values at low velocities exceed expected values based upon ground-state to ground-state energy defects, (c) extrapolated and actual total cross-section maxima occur at velocities corresponding to the smallest energy defect for each case, and (d) photon measurements show curve shapes similar to those of total cross sections in the near-adiabatic region.

Evidence of competition between final states is seen in these experimental results where the $\sigma(2p)$ cross section shows a shift toward lower velocity, and a more rapid decrease in the high velocity region than the total cross section as the competitive factor increases. The $\sigma(2p)$ maxima also become increasingly narrow as the competitive factor increases. Thus the increasing cross section for transfer to the ground state occurs with a corresponding decrease in the cross section for transfer to an excited state rather than the two independently contributing to the total nonresonant cross section which could cause it to exceed the incident atom resonant cross section.

ACKNOWLEDGMENTS

The authors express their thanks to R. C. Speiser and J. Duardo for their technical contributions, to J. R. Otto who assisted in setting up the apparatus, to D. Marines who provided filter transmission data, and to R. E. Olson of Stanford Research Institute for helpful discussions.

---

*Work supported by U. S. Army Research Office, Durham.

[1]J. B. Hasted, in *Advances in Electronics and Electron Physics*, edited by L. Marton (Academic, New York, 1960), Vol. 13, p. 1.

[2]H. S. W. Massey, Rept. Progr. Phys. 12, 248 (1949); H. S. W. Massey and E. H. S. Burhop, *Electronic and Ionic Impact Phenomena* (Clarendon, London, 1956), p. 441.

[3]D. Rapp and W. E. Francis, J. Chem. Phys. 37, 2631 (1962).

[4]J. Perel, R. H. Vernon, and H. L. Daley, Phys. Rev. 138, A937 (1965).

[5]J. Perel, R. H. Vernon, and H. L. Daley, in *Fourth International Conference on Physics of Electronic and Atomic Collisions, Quebec*, 1965 (Science Bookcrafters, Hastings-on-Hudson, N. Y., 1965), p. 336.

[6]J. Perel and A. Y. Yahiku, in *Fifth International Conference on Physics of Electronic and Atom Collisions, Leningrad*, 1967 (Nauka, Leningrad, 1967), p. 400.

[7]H. L. Daley and J. Perel, in *Sixth International Conference on the Physics of Electronic and Atomic Collisions, Cambridge*, 1969 (MIT Press, Cambridge, Mass., 1969), p. 1051.

[8]B. L. Donnally, T. Clapp, W. Sawyer, and M. Schultz, Phys. Rev. Letters 12, 502 (1964).

[9]I. A. Sellin and L. Granoff, Phys. Letters 25A, 484 (1967).

[10]A. S. Schlachter, P. J. Bjorkholm, D. H. Lloyd, L. W. Anderson, and W. Haeberli, Phys. Rev. 177, 184 (1969).

[11]J. R. Peterson and D. C. Lorents, Phys. Rev. 182, 152 (1969).

[12]A. S. Schlachter, D. H. Lloyd, P. J. Bjorkholm,

L. W. Anderson, and W. Haeberli, Phys. Rev. 174, 201 (1968).
[13]J. Perel and H. L. Daley, Bull. Am. Phys. Soc. 13, 614 (1968).
[14]J. Perel and H. L. Daley, Bull. Am. Phys. Soc. 14, 259 (1969).
[15]H. L. Daley and J. Perel, AIAA J. 7, 733 (1969).
[16]H. L. Daley and J. Perel, Bull. Am. Phys. Soc. 14, 1179 (1969).
[17]G. F. Drukarev, in Ref. 6, p. 10.
[18]D. V. Chkuaseli, A. I. Guldamashvilli, and V. D. Nikoleyishvilli, Bull. Acad. Sci. USSR 27, 976 (1963).
[19]L. L. Marino, Phys. Rev. 152, 46 (1966).
[20]L. L. Marino, *Atomic Collision Processes* (North-Holland, Amsterdam, 1964), p. 807.
[21]J. Perel and H. L. Daley, Bull. Am. Phys. Soc. 14, 1179 (1969).
[22]J. Perel and H. L. Daley, Bull. Am. Phys. Soc. 13, 1656 (1968).
[23]J. Perel and H. L. Daley, Ref. 7, p. 1055.
[24]L. I. Pivovar, L. I. Nikolaichuk, and A. N. Grigor Grigor'ev, Zh. Eksperim. i Teor. Fiz. 57, 432 (1969) [Sov. Phys. JETP 30, 236 (1970)].
[25]H. L. Daley and J. Perel (unpublished).
[26]H. R. Kaufman and P. D. Reader, in *AIAA Progress in Astronautics and Aeronautics: Electrostatic Propulsion*, edited by D. B. Langmuir, E. Stuhlinger, and J. M. Sellen, Jr. (Academic, New York, 1961), Vol. 5, p. 3.
[27]J. Perel, J. Electrochem. Soc. 115, 34C (1968).
[28]W. Bleakney, Phys. Rev. 35, 139 (1930).
[29]W. Ramsey (private communication).
[30]H. L. Daley, A. Y. Yahiku, and J. Perel, J. Chem. Phys. 52, 3577 (1970).
[31]J. Perel, Rev. Sci. Instr. 39, 394 (1968).
[32]J. Perel, H. L. Daley, and F. J. Smith, Phys. Rev. A 1, 1626 (1970).
[33]Notation taken from C. Candler, *Atomic Spectra* (Van Nostrand, Princeton, N. J., 1964).
[34]G. Herzberg, *Spectra of Diatomic Molecules* (Van Nostrand, Princeton, N. J., 1959), p. 267.

PHYSICAL REVIEW A VOLUME 4, NUMBER 1 JULY 1971

Low-Energy Elastic and Fine-Structure Excitation Scattering of Ground-State C^+ Ions by Hydrogen Atoms†

Jon C. Weisheit* and Neal F. Lane‡
Department of Physics, Rice University, Houston, Texas 77001
(Received 18 January 1971)

Cross sections are computed for the elastic and fine-structure excitation scattering of singly ionized carbon atoms by low-energy (less than 0.1 eV) hydrogen atoms. A close-coupling formulation is employed and the scattering equations are solved in a coupled-angular-momentum representation. The correct energy defect between the $C^+(^2P)$ fine-structure levels is included. For the first time, both spin-change and long-range electrostatic coupling terms are explicitly included in the scattering equations. The calculated C^+-H excitation cross section varies from 4.87×10^{-15} cm^2 at 0.01 eV to 2.86×10^{-15} cm^2 at 0.085 eV, and the maximum of almost 5.60×10^{-15} cm^2 occurs near 0.015 eV. The spin-change coupling, described herein, is found to be much more important than the long-range electrostatic coupling at all energies considered.

I. INTRODUCTION

Recent surveys[1,2] have emphasized the importance of heavy-particle collisions in astrophysics. In particular, calculations of the fine-structure excitation cross sections of $C(^3P)$, $C^+(^2P)$, $O(^3P)$, and $Si^+(^2P)$ atoms in collision with slow $H(^2S)$ atoms have indicated that in the interstellar medium these reactions have large rate coefficients.[3-8] Such collisional excitations and the subsequent forbidden radiative decays provide a significant cooling mechanism for interstellar gas.

Each of the theoretical investigations cited above has included the simplifying approximation that the excitation processes are elastic, i.e., that the energy differences between fine-structure levels are small in comparison with the center-of-mass kinetic energy of the colliding atoms and consequently may be neglected. Temperatures corresponding to the excitation energies ($\Delta T = \Delta E/k_B$, where k_B is the Boltzmann constant) of the C, C^+, O, Si, and Si^+ ground-state fine-structure levels range from 23 to 411 °K. It is evident that in interstellar space, where the temperature is typically 125 °K,[1] these fine-structure excitation collisions are highly inelastic events and thus the approximation of elastic scattering may be quite inappropriate. Furthermore, in all previous work the assumption has been made that the scattering is dominated entirely by the spin-change process[3,5,7,8] or by the orientation-dependent electrostatic interaction.[4,6] Up to the present time there have been no